Article

Comparisons of Spatial and Temporal Variations in PM$_{2.5}$-Bound Trace Elements in Urban and Rural Areas of South Korea, and Associated Potential Health Risks

Jayant Nirmalkar [1], Kwangyul Lee [2], Junyoung Ahn [3], Jiyi Lee [4] and Mijung Song [1,5,*]

[1] Department of Earth and Environmental Sciences, Jeonbuk National University, Jeonju 54896, Republic of Korea; jayant@jbnu.ac.kr
[2] Division of Climate and Air Quality Research, National Institute of Environmental Research, Chungcheong Region Air Quality Research Center, Seosan 32010, Republic of Korea
[3] Division of Climate and Air Quality Research, National Institute of Environmental Research, Incheon 22689, Republic of Korea
[4] Department of Environmental Science and Engineering, Ewha Womans University, Seoul 03760, Republic of Korea
[5] Department of Environment and Energy, Jeonbuk National University, Jeonju 54896, Republic of Korea
* Correspondence: mijung.song@jbnu.ac.kr

Abstract: PM$_{2.5}$-bound trace elements were chosen for health risk assessment because they have been linked to an increased risk of respiratory and cardiovascular illness. Since the Korean national air quality standard for ambient particulate matter is based on PM$_{2.5}$ mass concentration, there have only been a few measurements of PM$_{2.5}$ particles together with trace elements that can be utilized to evaluate their effects on air quality and human health. Thus, this study describes the trace elements bound to PM$_{2.5}$ in Seoul (urban area) and Seosan (rural area) using online nondestructive energy-dispersive X-ray fluorescence analysis from December 2020 to January 2021. At both the Seoul and Seosan sites, S, K, Si, Ca, and Fe constituted most of the PM$_{2.5}$-bound trace elements (~95%); major components such as S, K, and soil (estimatedcalculatedcalculated based on oxides of Si, Fe, Ca, and Ti) were presumably from anthropogenic and crustal sources, as well as favorable meteorological conditions. During winter, synoptic meteorology favored the transport of particles from severely contaminated regions, such as the East Asian outflow and local emissions. The total dry deposition flux for crustal elements was 894.5 ± 320.8 µg m^{-2} d^{-1} in Seoul and 1088.8 ± 302.4 µg m^{-2} d^{-1} in Seosan. Moreover, potential health risks from the trace elements were estimated. Cancer risk values for carcinogenic trace elements (Cr, As, Ni, and Pb) were within the tolerable limit (1×10^{-6}), suggesting that adults and children were not at risk of cancer throughout the study period in Seoul and Seosan. Furthermore, a potential risk assessment of human exposure to remaining carcinogens (Cr, As, Ni, and Pb) and non-carcinogens (Cu, Fe, Zn, V, Mn, and Se) indicated that these trace elements posed no health risks. Nevertheless, trace element monitoring, risk assessment, and mitigation must be strengthened throughout the study area to confirm that trace-element-related health effects remain harmless. Researchers and policymakers can use the database from this study on spatial and temporal variation to establish actions and plans in the future.

Keywords: PM$_{2.5}$-bound trace elements; dry deposition; hazard index; cancer risk assessment; origins

1. Introduction

Fine particulate matter (PM$_{2.5}$) plays a crucial role in determining visibility and affects climate change and human health [1–5]. Furthermore, the chemical components of PM$_{2.5}$ may be associated with a number of adverse health effects (e.g., respiratory diseases, cardiovascular disease, pregnancy/birth outcomes) [6–8].

In recent decades, PM$_{2.5}$ pollution has become a severe environmental concern in urban and rural areas in Asia [9–16]. Field measurements have shown that PM$_{2.5}$ is a

complex mixture of organic materials, inorganic salts, and trace elements [17–20]. Si, Fe, Ca, K, Ti, Cr, Mn, Zn, Ni, Cu, Pb, As, V, and Ba are significant contributors to $PM_{2.5}$-bound trace elements [21–24]. Their sources include regional aerosols, local road traffic, coal combustion, soil, and metal industries [4,10,25]. Due to their long residence time in the atmosphere, trace elements bound to $PM_{2.5}$ can be transported downwind [26]. Moreover, $PM_{2.5}$-bound trace metals may be deposited in terrestrial and aquatic ecosystems via the processes of dry deposition—which is a consistent and reliable atmospheric cleansing process—or wet deposition [27–29].

The health effects of trace elements must be addressed, because their potential carcinogenic and non-carcinogenic effects on human health have raised concerns [30–32]. As stated by the International Agency for Research in Cancer, trace metals such as Cd, Ni, Ar, Pb, and Cr can cause cancer in humans and animals [33–36]. When the CR is 10^{-4}, there is a serious risk of cancer. When the CR is between 10^{-6} and 10^{-4}, the risk is acceptable. When CR is 10^{-6}, there is less risk or the risk may be ignored [33,34]. Additionally, according to several epidemiological studies, $PM_{2.5}$ exposure has been associated with substantial health risks [37,38]. The complex characteristics of ambient $PM_{2.5}$ necessitate knowledge of its sources, sinks, and temporal and spatial variations. Trace elements can be utilized as markers for source apportionment studies of these particles, owing to their distinctive source characteristics.

Few studies on $PM_{2.5}$ and trace elements have compared urban and rural areas in South Korea [39–41]. To fill these gaps in $PM_{2.5}$ research, we conducted simultaneous $PM_{2.5}$ monitoring studies at representative sites in the urban (Seoul) and rural (Seosan) regions of South Korea during the winter season. Seoul is affected by local anthropogenic emissions and regional outflows that cause high $PM_{2.5}$ concentrations [42]. Seosan was chosen based on recent studies that found high $PM_{2.5}$ concentrations in the area. However, the causes of this are yet to be known [42,43]. In this study, we evaluated the temporal and spatial variability of $PM_{2.5}$ and trace elements, along with their possible health risks to humans throughout the winter of 2020–2021 at rural and urban sites. The findings concerning trace elements, their sources, and their estimated potential risks to humans in Seoul (urban) and Seosan (rural) will have important implications for controlling air pollution and improving wellbeing. This research strengthens the existing research by estimating potential health risks in the context of comparing two different locations in South Korea and similar locations worldwide.

2. Materials and Methods

2.1. Study Site

Simultaneous measurements were conducted in Seoul (urban area) and Seosan (rural area) from 15 December 2020 to 15 January 2021. Seoul and Seosan are approximately ~99 km apart. Seoul is a city with a population of approximately 10 million and an area of 605 km^2 (Figure S1) [44]. The measurements in Seoul were performed at an air-quality measurement site run by the National Institute of Environmental Research (NIER) in the metropolitan area of Bulgwang-dong, Eunpyeong-gu, Seoul (37.61° N, 126.93° E). The site is surrounded by many highly congested roads and residential complexes [44–46].

Seosan is a rural area in Chungcheong-do with a population of approximately 0.18 million and an area of 742 km^2 (Figure S1) [43,46]. This area is considered an "agro-industrial area", which combines farms, power plants, and markets. The measurements were conducted at an air-quality monitoring station in the Chungcheong region operated by the NIER (36°78′ N, 126°49′ E).

2.2. Measurements

The concentrations of $PM_{2.5}$ and $PM_{2.5}$-bound trace elements were simultaneously quantified hourly at the two sites from 15 December 2020 to 15 January 2021. The β-ray absorption technique was used to measure the mass concentrations of $PM_{2.5}$ (BAM1020, Met One Instruments Inc., Grants Pass, OR, USA). Si, K, S, Ca, Ti, Fe, V, Mn, Cr, Ni,

Cu, As, Zn, Se, Ba, Br, and Pb were quantified using an ambient online nondestructive energy-dispersive X-ray fluorescence monitor (Xact625i, Ambient Metal Monitor, COOPER ENVIRONMENTAL, Tigard, OR, USA) [47,48]. The method detection limit (MDL) varied from 1.17 to 17.8 ng m^{-3} for Si, S, Cl, and K (Table S1), [47,49,50] and from 0.1 to 0.39 ng m^{-3} for Ba, Ca, Fe, Mn, Pb, V, Cr, Ni, and Br. For Se, Cu, Zn, and As, the MDL ranged from 0.063 to 0.08 ng m^{-3} [49,50]. A high percentage of samples were below the detection limit for Ba, Ni, and V in Seoul, and for V, Si, and Cr in Seosan (Table 1).

Table 1. Summary statistics of trace element concentrations (ng m^{-3}) in PM$_{2.5}$ quantified in Seoul and Seosan, South Korea, from 15 December 2020 to 15 January 2021.

	Seoul			Seosan		
Element	**Mean ± SD [a]**	**% BDL [b]**	**Median**	**Mean ± SD**	**%BDL**	**Median**
Si	306 ± 527	30	101	460 ± 761	47	147
S	1444 ± 908	0.9	1168	1265 ± 673	2.3	1153
K	250 ± 131	0.9	219	294 ± 203	2.2	239
Ca	81 ± 113	0.9	47	101 ± 160	2.2	53.0
Ti	10.6 ± 10	0.9	7.8	12 ± 15	2.2	6.6
V	0.7 ± 0.5	33	0.5	0.7 ± 0.7	56	0.4
Cr	1.2 ± 1.0	7.7	0.9	1.3 ± 1.4	17	0.8
Mn	13 ± 8.2	0.9	11	16 ± 22	2.6	10
Fe	183 ± 135	1.0	142	210 ± 201	2.2	153
Ni	0.8 ± 0.7	58	0.7	0.7 ± 0.8	12.6	0.4
Cu	4.4 ± 4.0	0.9	2.9	4.1 ± 4.0	3.4	3.1
Zn	49 ± 85	0.9	37	51 ± 41	2.6	39
As	4.7 ± 3.8	0.9	3.8	3.9 ± 3.3	3.3	3.1
Se	1.0 ± 1.0	7.4	0.5	1.4 ± 1.4	7.9	1.0
Br	7.3 ± 6.4	0.9	4.8	8.8 ± 6.2	2.3	7.5
Ba	2.2 ± 1.8	61	1.7	-	−100	-
Pb	21 ± 11	0.9	19	21.0 ± 11.8	4.3	19.7
Temperature (°C)	−3.5 ± 6.3	-	-	−2.64 ± 5.63	-	-
Relative humidity (%)	56.9 ± 15.7	-	-	70.0 ± 17.1	-	-
Wind speed (m/s)	2.38 ± 1.09	-	-	1.79 ± 1.67	-	-
Wind direction (degree)	205 ± 110.1	-	-	146 ± 138	-	-
Rainfall (mm)	0.76 ± 0.93	-	-	0.33 ± 0.25	-	-

[a] Standard deviation; [b] below detection limit.

2.2.1. Dry Deposition Calculations

Dry deposition flux (DDF) is calculated by multiplying element concentrations by dry deposition velocities [24,51]. DDFs (μg m^{-2} d^{-1}) of trace elements were estimated for the Seoul and Seosan sites. Herein, the dry deposition rates of specific species were expected to be 2 cm s^{-1} for dust-originated elements, 1 cm s^{-1} for anthropogenic elements, and 0.5 cm s^{-1} for remaining trace elements; these were selected based on previous research on these species of PM$_{2.5}$ [24,52–54]. In prior works, similar dry deposition rates were estimated using the DDF of atmospheric trace elements [24,55].

2.2.2. Exposure Estimations

Non-carcinogenic and carcinogenic health risk assessments for trace elements (Figure S4) were conducted using the methods of the Integrated Risk Information System and the United States Environmental Protection Agency database [56–59]. PM$_{2.5}$-bound trace elements pose potential health risks to children and adults through dermal contact, inhalation, and ingestion; therefore, the dermal absorbed dose (DAD), chemical daily intake (CDI), and exposure concentration (EC) were assessed [59] (Equations (1)–(3), respectively). The exposure assessment formulae are as follows:

$$\mathrm{DAD_{dermal}} = \frac{\mathrm{C \times SA \times AF \times ABS}}{\mathrm{BW}} \times \frac{\mathrm{EF \times ED}}{\mathrm{AT}} \times \mathrm{CF}, \qquad (1)$$

$$\mathrm{CDI_{ingestion}} = \frac{\mathrm{C \times IngR}}{\mathrm{BW}} \times \frac{\mathrm{EF \times ED}}{\mathrm{AT}} \times \mathrm{CF}, \tag{2}$$

$$\mathrm{EC_{inhalation}} = \mathrm{C} \times \frac{\mathrm{InhR \times EF \times ED}}{\mathrm{BW \times PEF \times ATn}}, \tag{3}$$

where C is the concentration ($\mu g\ m^{-3}$). The exposure duration (ED) is 6 y for children and 24 y for adults. IngR is the ingestion rate ($mg\ day^{-1}$), and EF is the exposure frequency (180 d y^{-1} for residents). The ingestion rate is 200 and 100 mg d^{-1} for children and adults, respectively. Body weight (BW) is 70 and 15 kg for adults and children, respectively; CF (conversion factor) is 10^{-6} kg mg^{-1}; ET (exposure time) is 24 h d^{-1}; AT (the time average for non-carcinogenic elements) is equal to ED $\times$ 365 days, where for carcinogens it is equal to 70 years $\times$ 365 days [24,59,60] (Table S2). The average time (ATn) for non-carcinogens is ATn = 365 d $\times$ ED $\times$ 24 h d^{-1}, while for carcinogenic elements is ATn = 70 y $\times$ 24 h $\times$ 365 d y^{-1}. AF (the skin adherence factor) is 0.2 mg $cm^{-1}\ h^{-1}$; SA denotes the exposed skin area (3300 and 2800 cm^2 for adults and children, respectively). According to the US EPA, the dermal absorption factor (or ABS) is 0.03, 0.1, and 0.01 for As, Pb, and the remaining elements, respectively (Table S2) [24,59,61].

2.2.3. Non-Carcinogenic Risk Characterizations

To calculate non-carcinogenic risks, we used the hazard index (HI = ΣHazard Quotient (HQ). The non-CR caused by $PM_{2.5}$-bound trace elements (Cr, Mn, Ni, Cu, V, Zn, As, and Pb) was determined utilizing the following equations (Equations (4)–(7)):

$$\mathrm{HQ_{ingestion}} = \frac{\mathrm{CDI}}{\mathrm{RfDo}}, \tag{4}$$

$$\mathrm{HQ_{dermal}} = \frac{\mathrm{DAD}}{\mathrm{RfDo * GIABS}}, \tag{5}$$

$$\mathrm{HQ_{inhalation}} = \frac{\mathrm{EC}}{RfCi * 1000\ \mu g\ mg^{-1}}, \tag{6}$$

$$\mathrm{HI = HQ_{ingestion} + HQ_{dermal} + HQ_{inhalation}}, \tag{7}$$

where the oral reference dosage is in mg $kg^{-1}\ d^{-1}$, while the gastrointestinal absorption factor and the inhalation reference concentration are in $\mu g\ m^{-3}$, and they are denoted by RfDo, GIABS, and RfCi, respectively (Table S2). The probable non-cancer consequences were measured using the HI, estimated as the sum of the HQ values [57,60,62]. When the HI values of non-carcinogenic trace elements were below one, they did not pose a risk to adults or children [56]. The potential for non-carcinogenic risks increases if the HI increases above one [59].

2.2.4. Cancer Risk Characterizations

CR is the likelihood of developing cancer due to lifelong contact with carcinogens [10]. Intended for regulatory purposes, the acceptable or tolerable hazard of emerging cancer throughout of a human's life ranges from 1×10^{-4} to 1×10^{-6} [63]. The CR posed by trace elements (Cr, Ni, As, and Pb) through various paths—including inhalation, ingestion, and dermal contact—was estimated and used to calculate the total cancer hazard (CR_{risk}) as follows (Equations (8)–(11)) [56,59]:

$$\mathrm{CR_{ingestion}} = \frac{\mathrm{CDI}}{\mathrm{SF0}}, \tag{8}$$

$$\mathrm{CR_{dermal}} = \frac{\mathrm{DAD}}{\mathrm{SF0 * GIABS}}, \tag{9}$$

$$CR_{inhalation} = IUR * EC, \tag{10}$$

$$CR_{risk} = CR_{ingestion} + CR_{dermal} + CR_{inhalation}, \tag{11}$$

where the inhalation unit risk is in $\mu g\ m^{-3}$, the inhalation reference concentration is in $\mu g\ m^{-3}$, and the oral slope factor is in $mg\ kg^{-1}\ d^{-1}$, denoted by IUR, RfCi, and SFo, respectively. A CR of greater than 10^{-4} indicates a severe risk of cancer [64]. In contrast, a CR of less than 10^{-6} indicates either a low risk or an acceptable risk [64]. Previous research has determined that the concentration proportion of Cr(VI) and Cr(III) is 1:6. As a result, the Cr(VI) concentration used to calculate the CR was adjusted to 1/7 of the total Cr concentration observed [24].

2.2.5. Principal Component Analysis (PCA)

Principal component analysis (PCA) was used in the Origin application (OriginPro, Version 2022, OriginLab Corporation, Northampton, MA, USA) to identify potential sources of $PM_{2.5}$-bound trace elements in Seoul and Seosan. PCA was used to identify site-specific sources using winter data by site [65,66]. PCA was performed using a varimax rotation of the data matrix, and the principal components (PCs) or factors (Fs) were extracted in accordance with a set of quality criteria: the number of eigenvalues greater than 1 (Kaiser criterion), with more than 70–85% of cumulative variance explained by the corresponding PCs. The loadings of obvious variables were near one, while those of non-obvious variables were near zero. Variables with a loading of 0.5 were considered to be factor indicators.

2.2.6. Enrichment Factor

The enrichment factors (EFs) were calculated in order to determine the degree of contamination of each element in $PM_{2.5}$, and to determine whether it primarily came from anthropogenic or natural sources [44,67]. The definition of EF is the ratio of a particular element's concentration (X_i) to Fe ($X_{reference}$, a reference element for crustal dust), normalized to the same ratio in the upper continental crust and calculated as follows using Equation (12) [68]:

$$\text{Enrichment Factors} = \frac{\left(\frac{X_i}{X_{reference}}\right)_{Aerosol}}{\left(\frac{X_i}{X_{reference}}\right)_{Crust}} \tag{12}$$

where ()aerosol and ()crust refer to the $PM_{2.5}$ sample and continental crust, respectively. The reference element used in this study was iron (Fe), which is also supported by previous research in Korea [44].

2.2.7. Potential Source Contribution Function (PSCF)

The PSCF was calculated using $PM_{2.5}$-bound trace element concentrations, and air-mass back-trajectories were calculated using NOAA's HYSPLIT4 (Hybrid Single-Particle Lagrangian Trajectory) model with Global Data Assimilation System (GDAS) grid meteorological data to identify the likely locations of the regional sources for long-range transboundary aerosols [69,70]. This calculates the probability that a source exists at latitude i and longitude j. The PSCF for the ijth grid cell, $PSCF_{ij}$, was determined for $PM_{2.5}$ values as follows:

$$PSCF_{ij} = \frac{m_{iij}}{n_{ij}} \tag{13}$$

where n_{ij} is the total number of trajectory endpoints that fall into the ijth cell, and m_{ij} is the number of endpoints in the same cell corresponding to trajectories associated with concentration values at each receptor site above a predefined criteria value [70]. As a result, cells with a high PSCF value are expected to produce high concentration values at receptor locations and, thus, can be reasonably believed to be potential source areas [69]. The details of the PSCF input parameters are given elsewhere [70].

2.2.8. Tukey's Test and Paired *t*-Test

The daily mean concentrations of $PM_{2.5}$ and $PM_{2.5}$-bound trace elements between Seoul and Seosan were compared using one-way analysis of variance (ANOVA) with Tukey's test and paired *t*-tests [71,72]. These tests were carried out to determine whether there were any significant differences in the mean $PM_{2.5}$ and $PM_{2.5}$-bound trace element concentrations between the Seoul and Seosan sites. The paired-sample *t*-test's statistical significance level was set at 5%.

3. Results and Discussion

3.1. Overview of Trace Elements and $PM_{2.5}$ in Urban and Rural Areas

During the present study, in Seoul, S had the highest median concentration of all trace elements in $PM_{2.5}$ (1446.9 ng m^{-3}), followed by K (251.1 ng m^{-3}) and Si (237.5 ng m^{-3}); in Seosan, S also had the highest median concentration (1265.2 ng m^{-3}), followed by Si (306.1 ng m^{-3}) and K (294.5 ng m^{-3}) (Table 1). For all elements, the mean concentrations were higher than the median concentrations, indicating the impact of episodic high-concentration events (Table 1). A similar variance in mean and median concentrations has been reported in Bhopal, India, possibly as a result of the impact of episodic high-concentration events [24]. Furthermore, $PM_{2.5}$ concentrations were higher than 35 µg m^{-3} during episodic events, owing to high concentrations of S, K, and crustal elements at both study sites (Figure S2). In Seoul, the mean concentrations for Ni and S varied between 0.5 ng m^{-3} and 1446.9 ng m^{-3}, while those for V and S in Seosan varied between 0.51 ng m^{-3} and 1265.2 ng m^{-3}. S and crustal elements (Si, Ca, and Fe) were the major components detected in both Seoul and Seosan, which is consistent with the findings of previous studies conducted at these locations during winter [19,39]. The mean S concentration was significantly higher in Seoul than in Seosan, and the opposite trend was true for the concentrations of crustal elements (Si, Fe, Ca, and Ti). The paired *t*-test revealed that the differences between Seoul and Seosan based on S, K, Ca, and Fe were statistically significant (Tukey's test and paired *t*-test, *p* < 0.05; Table S4). In Seoul, high S concentrations were primarily emitted from burning coal [73]. The higher crustal element concentrations in Seosan compared with those in Seoul may have been due to the characteristics and amounts of resuspended dust. K concentrations were higher in Seosan than in Seoul, which could be attributed to wood burning for cooking and agricultural waste burning to prepare fields for the next harvest.

Anthropogenic elements, such as Zn, Pb, Mn, Cu, and As, were prevalent at both sites. The concentrations of Pb, Cu, V, Ni, Se, and Zn at both sites were similar. Zn and Cu are tracers of brake and tire wear [74]. The primary sources of atmospheric Pb in previous studies have been identified as vehicular and ship emissions, heavy oil combustion, transboundary coal combustion emissions, waste incineration, and recirculation of historic leaded gasoline [74]. Moreover, Fe, Pb, and Zn emissions in China in 2013 were determined to have originated from five main emission sectors: industrial, residential sources, transportation, power generation, and windblown dust [75].

Trace elemental ratios are reliable tracers of pollutants emitted to the atmosphere by coal combustion, oil combustion, waste burning, and industrial emissions [74,76,77]. As tracers for coal and oil combustion, respectively, the V/Pb and V/Ni ratios can be used [78]. In general, coals have a high V content, and a V/Pb ratio greater than 1 suggests coal combustion emissions, while a lower V/Pb ratio implies vehicle exhaust emissions. The waste and emissions from non-coal-burning industries have a V/Pb ratio of <<1. The ratios of V/Pb were found to be 0.03 ± 0.03 in Seoul and 0.03 ± 0.04 in Seosan. The V/Pb ratio was <<1, indicating that these elements may be emitted as a result of industrial activity or the burning of waste. The impurities V and Ni have been widely used as tracers of petroleum combustion, since they are always present in heavy oil [79]. The V/Ni ratio in heavy oil combustion is between 3 and 4, the ratio in ship emissions is between 2.5 and 5, and increased Ni emissions from oil burning result in lower ratios [74,80–82]. The V/Ni ratio was found to be 1.33 ± 2.08 in Seoul and 1.04 ± 1.17 in Seosan, suggesting that these

elements may be emitted during oil combustion. The V/Ni ratios of above 0.7 suggested that these elements were emitted as a result of oil burning [82].

During the entire monitoring period, the daily mean concentration of $PM_{2.5}$ in Seosan (31.2 ± 13.3 μgm^{-3}) was higher than that in Seoul (23.0 ± 12.4 μgm^{-3}) [42] (Text S1). During the study period, the daily mean values of temperature (T), relative humidity (RH), and wind speed (WS) were -3.5 ± 6.3 °C, $57 \pm 16\%$, and 2.4 ± 1.1 m s^{-1} in Seoul, respectively, and -2.6 ± 5.6, $70 \pm 17.1\%$, and 1.8 ± 1.7 m s^{-1} in Seosan, respectively. In comparison to the Seoul site, Seosan had a higher relative humidity and a lower wind speed. The higher $PM_{2.5}$ concentrations in Seoul compared to Seosan were mostly attributable to the lower temperature, lower wind speed, and higher relative humidity during the measurement period [42]. According to previous studies, high $PM_{2.5}$ concentrations result from its accumulation under high RH, low WS, and low T [42,83–85].

3.2. Comparison of Variation in the Trace Elements of $PM_{2.5}$ in Urban and Rural Areas

The diurnal variation in $PM_{2.5}$-bound trace elements is important because it suggests information about the short-term air quality, sources, and formation characteristics of these components on an hourly basis [26]. Figure 1 displays the diurnal variations in $PM_{2.5}$ and its trace elements in Seoul (dashed black line) throughout the entire measurement period. The main peak in hourly $PM_{2.5}$ concentration in Seoul occurred between 9:00 and 14:00 (Figure 1). S displayed a high concentration between 5:00 and 13:00, and a second peak between 15:00 and 20:00. In Seoul, no apparent diurnal variations in K concentrations were observed. The Si, Fe, Ca, and Ti concentrations peaked between 7:00 and 14:00, which may be associated with crustal sources. Because of potential similarities in their sources, Cu, Pb, Zn, and Mn also showed concentration peaks between 7:00 and 14:00. The Br concentration peaked around 10:00 and 19:00 at the Seoul site.

Figure 1 shows the diurnal variation in $PM_{2.5}$ and its elements in Seosan (red solid line). A bimodal distribution of hourly $PM_{2.5}$ concentrations was observed, with a major peak between 20:00 and 22:00, and a comparable peak between 8:00 and 13:00 (Figure 1). S showed a high concentration peak between 8:00 and 14:00, followed by modest peaks at 16:00–18:00 and 20:00–23:00. K demonstrated an intense concentration peak between 8:00 and 14:00. Si, Ca, Fe, and Ti all showed high peaks between 9:00 and 14:00, which could be attributed to the similar sources of these elements. Zn, Cu, Pb, and Mn all showed major concentration peaks between similar hours of 9:00 and 14:00, which may also be indicative of similar origins. The Br concentration peaked around 10:00 and 22:00 at the Seosan site.

In general, almost all measured elements' concentrations increased in the morning and decreased in the afternoon in both the rural and urban areas (Figure 1). The morning peak could be attributed to vehicle emissions during traffic rush hours [86]. The peak concentrations of Cu, Zn, Mn, and Pb might be related to tire and brake-lining wear [87–89]. Source apportionment studies of Korea have suggested that Br and Pb may be emitted from vehicular and/or burning (e.g., biomass, waste material, coal, oil) activities [90,91]. However, the nighttime peak may have been due to decreases in T, WS, and planetary boundary layer height (PBLH), along with an increase in relative humidity (RH). At night, the lower PBLH tends to limit the dispersion of PM [92]. The PBLH was typically high during the day, which is suitable for pollution dispersion; thus, $PM_{2.5}$ and most elements displayed lower concentrations during the afternoon [92,93]. Furthermore, S had higher hourly concentrations in Seoul than in Seosan; however, the remaining trace elements had higher concentrations in Seosan than in Seoul. A more intense morning peak in K concentration was observed in Seosan than in Seoul, possibly due to agricultural burning activities in the rural area [43,94]. At both sites, Cr, As, Ni, V, and Se displayed clear peaks throughout the day, possibly owing to industrial emissions [95].
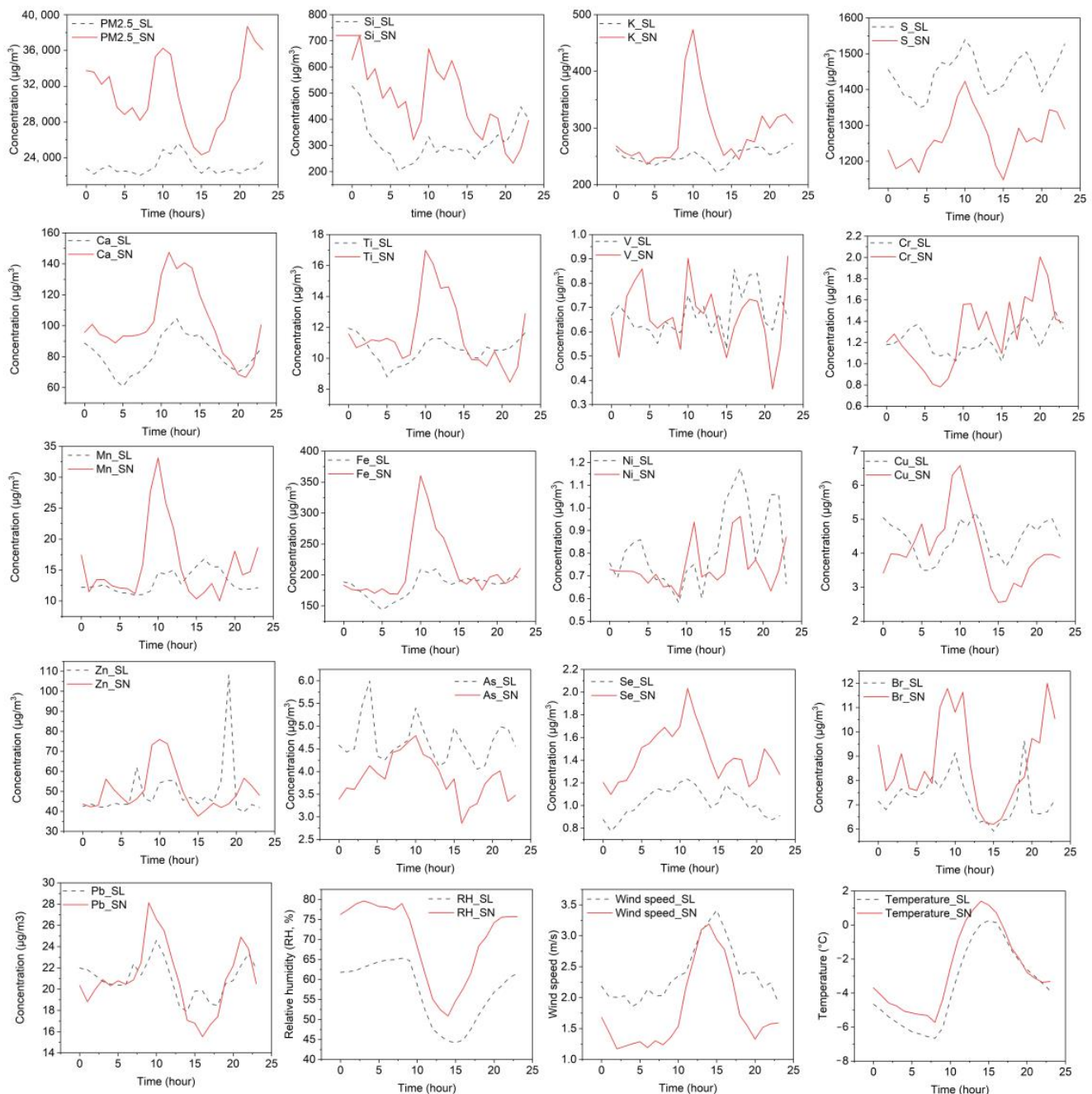
Figure 1. Hourly variations in concentrations of PM$_{2.5}$, elements, and meteorological parameters in Seoul (SL) and Seosan (SN) during winter.

3.3. Origins of Trace Elements in PM$_{2.5}$

Principal component analysis (PCA) was used to identify the sources of PM$_{2.5}$-bound trace elements at the Seoul and Seosan sites (Table 2, Text S2). PCA is widely used in studies to identify the sources of various aerosol components [10,44,96]. The factor loadings (F1 to F4) were determined using a varimax rotation for each element [97]. The number of factors was determined by an eigenvalue of one or more [97]. In this study, the three factors identified in Seoul and four in Seosan are described as follows:

Table 2. Varimax-rotated principal factor (F) loadings for $PM_{2.5}$-bound trace elements at the Seoul and Seosan sites during the winter period.

	Seoul			Seosan			
	F1	F2	F3	F1	F2	F3	F4
Si	0.01	0.98	−0.09	0.98	0.03	0.12	0.02
S	0.87	0.17	0.20	−0.11	0.88	0.25	0.07
K	0.55	0.68	0.34	0.58	0.64	0.31	0.10
Ca	0.03	0.98	−0.09	0.94	0.06	0.12	−0.09
Ti	0.09	0.98	−0.03	0.97	0.04	0.16	0.03
V	0.31	0.91	−0.08	0.83	0.29	0.02	0.23
Cr	0.88	0.36	0.17	0.46	0.52	0.44	−0.20
Mn	0.72	0.56	0.22	0.14	0.20	0.86	0.04
Fe	0.41	0.90	0.00	0.89	0.23	0.37	−0.03
Ni	0.81	0.31	0.16	0.50	0.81	0.05	−0.02
Cu	0.85	0.28	0.03	0.30	0.17	0.77	−0.05
Zn	0.62	−0.01	0.01	0.11	0.29	0.90	0.08
As	0.02	−0.13	0.95	0.05	−0.18	0.00	0.93
Se	0.87	0.27	0.05	0.13	0.88	0.21	−0.17
Br	0.95	0.14	−0.07	0.12	0.87	0.31	−0.01
Ba	0.70	−0.25	0.14	No data	No data	No data	No data
Pb	0.27	−0.01	0.93	0.04	0.33	0.61	0.59
Variance	9.05	3.76	1.69	7.94	3.02	1.78	1.16
Percentage of variance (%)	53.2	22.1	9.95	49.6	18.8	11.1	7.26
Cumulative (%)	53.2	75.3	85.3	49.6	68.5	79.6	86.8

F = factor.

Three factors contributed 85.3% of the total explained variation in the Seoul data. The first factor was anthropogenic activity (e.g., coal burning, industrial, biomass burning, and vehicular activities), with high S, Mn, Ni, Cu, Se, Br, Zn, and Ba loadings. The second factor was related to soil dust resuspension, with a high loading of crustal elements (Si, Ca, Ti, and Fe). The third factor revealed the presence of Pb and As sources, which included metal smelting, crustal sources, coal combustion, and burning of municipal waste [98–100].

Four factors contributed approximately 86.8% of the total variance in the Seosan data (Table 2). The first factor was the resuspension of soil dust, which had high loadings of crustal elements (Si, Ca, Ti, and Fe) (Table 2). The second factor had high loadings of S, K, Ni, Se, and Br, which were determined to be associated with coal and biomass burning. The third factor, characterized by high Cr, Mn, Cu, and Zn loadings, was related to traffic and industry. The fourth factor in Seosan was the high loadings of As and Pb. According to the analysis, K was mainly associated with crustal sources in Seoul and combustion sources in Seosan. As previously reported, V and Ni are well-known tracers for oil combustion sources [101]. However, in the PCA results, Ni and V were separate factors. Thus, source apportionment tools, such as positive matrix factorization (PMF), may be required to gain a better understanding of the sources of Ni and V in $PM_{2.5}$ sources in Seoul and Seosan.

Emissions from anthropogenic sources must be drastically reduced to the greatest extent practicable in comparison to emissions from natural sources. More important information for risk management can be obtained around the sampling site from a thorough assessment of the risk levels of metals from anthropogenic sources than from that of metals from natural sources (Figure 2). If the calculated values of EF for a certain element are close to unity, it means that crustal dust is the predominant source [67,102]. On the other hand, EFs greater than 10 suggest a considerable contribution from anthropogenic sources [67,74,103]. At both the Seoul and Seosan sites, S, Cu, Zn, As, Se, Br, and Pb were identified as anthropogenic elements with EF values greater than 10 (Figure 2). In a previous study conducted in Seoul, Si, Ti, and Fe were suggested as having crustal origins, while S, Zn, and Pb were suggested as anthropogenic elements using EF calculations [39].
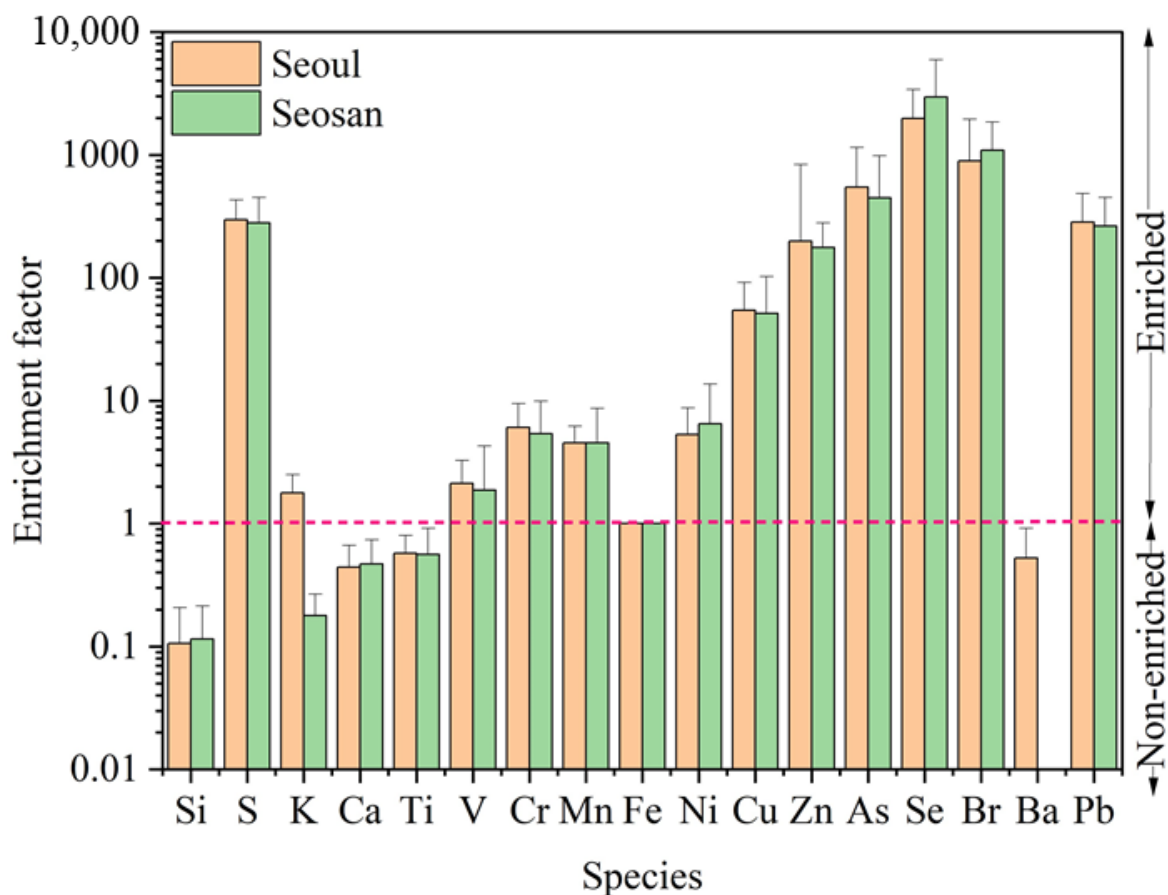
Figure 2. Enrichment factors of elements in $PM_{2.5}$ at the Seoul and Seosan sites (the variable of the Y-axis is in $\log_{10}$ scale).

To explore the possible source locations of $PM_{2.5}$ and its elements, the potential source contribution function (PSCF) was used (Figure 3a,b and Text S2). Text S2 in the Supplementary Materials provides information about backward air-mass trajectories and their use for PSCF. The results indicate that Southern China (i.e., Shandong, Anhui, Jiangsu, Henan, and Hebei provinces) was the likely source of $PM_{2.5}$ arriving at Seoul (Figure 3a), whereas that arriving at Seosan mainly originated from Jiangsu, Henan, and Anhui. Shandong, Anhui, Jiangsu, Henan, and Hebei were probable sulfur source locations for both sites. Industry in China has become more concentrated and agglomerated along the coast in the east, north, and south; Shandong, Anhui, Jiangsu, Henan, and Hebei are notable examples [104,105]. For K, the potential source locations for Seoul included Shandong, Jiangsu, and Hebei, whereas those for Seosan were the Jiangsu, Anhui, and Shanghai metropolitan areas. According to a previous study, the eastern provinces of China (including Shandong, Jiangsu, Hebei, Anhui, and Shanghai) are well known for their high $PM_{2.5}$ concentrations and biomass burning throughout the winter [106,107]. The fires were visible during the study period in the eastern regions of China (Figure S3). For soil, potential source regions for Seoul included Shandong, Jiangsu, and Hebei, whereas those for Seosan included Inner Mongolia and the coasts of Jiangsu, Anhui, and Zhejiang provinces.
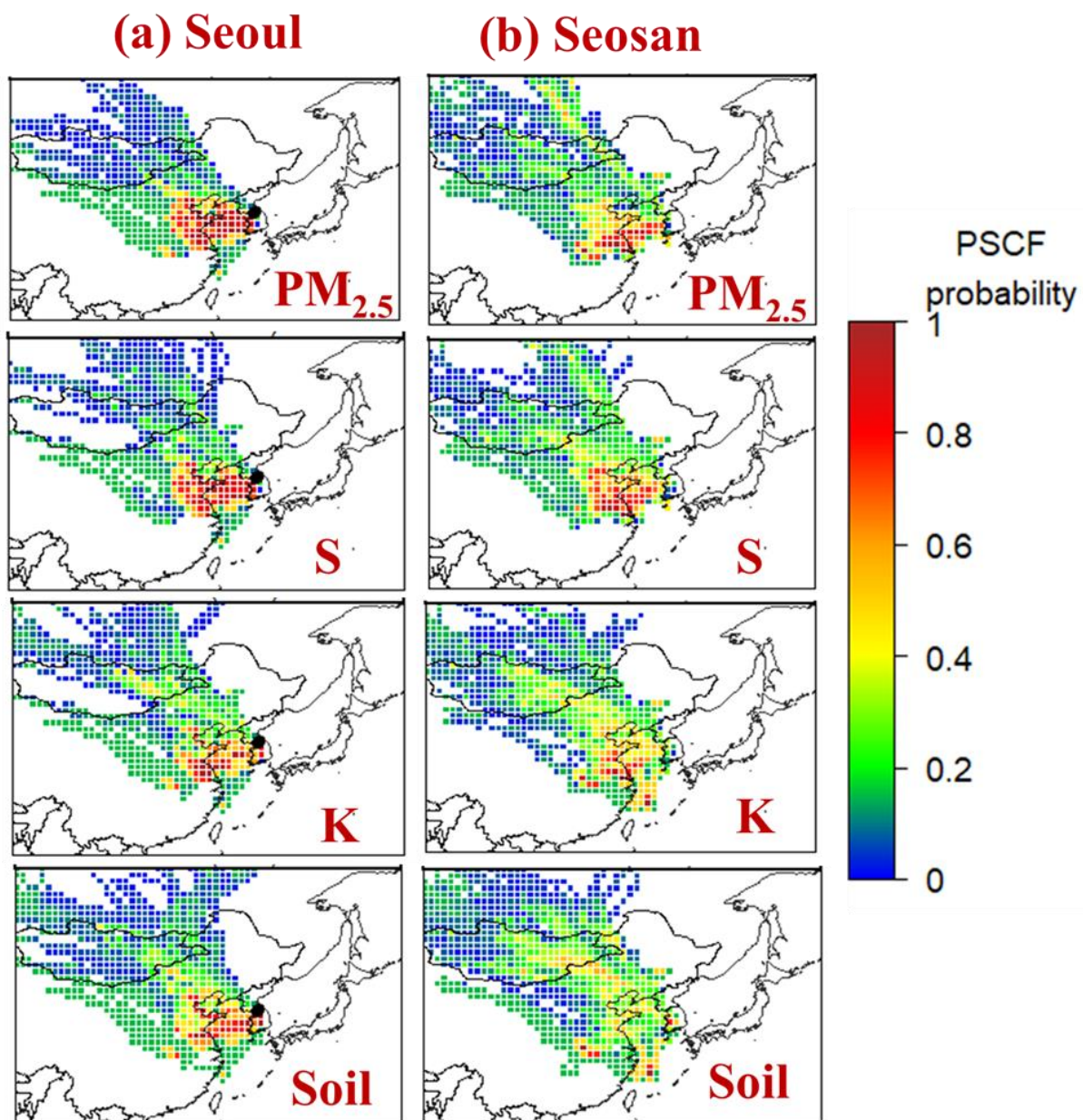
Figure 3. Potential source contribution function values for PM$_{2.5}$, S, K, and soil throughout the study period in (**a**) Seoul and (**b**) Seosan, South Korea, during winter.

3.4. Estimated Dry Deposition Fluxes of Elements in PM$_{2.5}$ in Urban and Rural Areas

Elements—especially metals that are toxic and deposited on soil and plants—can harm human health and the environment due to their entry and accumulation in food chains [53,108]. The atmospheric deposition of pollutants, which is known as dry deposition, can be measured as DDF and is a vital method for removing contaminants from the air [53,55,109]. Table 3 summarizes the average DDF for each element of PM$_{2.5}$ at the urban and rural sites. The average DDF values were within similar ranges at the two sites: from 0.5 ± 0.4 (Ni and V) to 1253.8 ± 654.0 µg m^{-2} d^{-1} (S) in Seoul, and from 0.3 ± 0.4 (V) to 1096.4 ± 451.6 µg m^{-2} d^{-1} (S) in Seosan (Table 3). The DDF values of S and primarily crustal elements (Si, Ca, and Fe) were higher than those of primarily anthropogenic elements (including, but not limited to, Mn, Zn, Cu, and Pb) for all samples at these study sites (Table 3).

Table 3. Average dry deposition flux (μg m^{-2} d^{-1}) for PM$_{2.5}$-bound elements in Seoul and Seosan during the winter period.

Element	Dry Deposition Velocity (cm s^{-1})	Mean $\pm$ SD (Seoul)	Mean $\pm$ SD (Seosan)
Si	2.0	411.6 $\pm$ 689.9	530.5 $\pm$ 801.8
S	1.0	1253.8 $\pm$ 654.0	1096.4 $\pm$ 451.6
K	2.0	435.2 $\pm$ 169.5	510.4 $\pm$ 194.8
Ca	2.0	144.3 $\pm$ 172.6	175.2 $\pm$ 219.8
Ti	2.0	18.6 $\pm$ 16.1	20.0 $\pm$ 18.7
V	1.0	0.5 $\pm$ 0.3	0.4 $\pm$ 0.4
Cr	0.5	1.0 $\pm$ 0.6	1.0 $\pm$ 0.6
Mn	1.0	11.4 $\pm$ 5.2	13.7 $\pm$ 10.4
Fe	2.0	319.9 $\pm$ 208.3	363.2 $\pm$ 242.3
Ni	0.5	0.5 $\pm$ 0.4	0.6 $\pm$ 0.4
Cu	0.5	1.9 $\pm$ 1.3	1.8 $\pm$ 0.9
Zn	0.5	21.3 $\pm$ 11.9	21.9 $\pm$ 9.6
As	0.5	2.0 $\pm$ 0.8	1.7 $\pm$ 0.7
Se	0.5	0.4 $\pm$ 0.4	0.6 $\pm$ 0.4
Br	0.5	3.2 $\pm$ 1.8	3.8 $\pm$ 1.5
Ba	0.5	0.7 $\pm$ 0.4	0.0 $\pm$ 0.0
Pb	0.5	9.1 $\pm$ 2.7	9.1 $\pm$ 2.5

The DDF values of crustal elements (such as Si, Ca, Fe, and Ti) were higher than those of anthropogenic elements (such as Zn, Pb, Mn, Cu, and As) at both locations, because crustal elements were generally found in bare soils and contributed to fine PM mass via resuspension during the study period [24,110,111]. According to prior research, even though heavy trace metals form a small fraction of particle mass and have lower DDFs than crustal elements, they are hazardous to both adults and children [12,112]. The standard deviations were comparable to or slightly greater than the mean DDF values, indicating significant daily variability in DDF (Table 3).

The similar dry deposition velocities at the Seoul and Seosan sites demonstrated that the DDF was controlled primarily by element concentrations, and the DDFs of pollutants were affected by their concentrations. Thus, the measured fluxes and concentrations should theoretically exhibit strong correlations [113,114]. In theory, particles with minimal changes in their DDF should have a strong association between their concentration and flux, because changes in concentration mainly affect flux [51,110]. Additionally, the RH was higher in Seosan (mean 70%) than in Seoul (57%), which might have played a role in the higher DDF for major elements in Seosan than for those in Seoul (Table 3). Furthermore, high RH results in increased particle size via hygroscopic growth, which can significantly increase the particle deposition rate [51].

3.5. Health Risk Assessments

3.5.1. Exposure Assessments for Trace Elements

The values for CDI, DAD, and EC correspond to ingestion, dermal contact, and inhalation, respectively, as shown in Figure S4. During the study period, adults and children in Seoul and Seosan were mainly exposed to trace elements through ingestion. The potential exposure of adults and children at both sites to S, K, and Si was higher via all three routes than for the remaining elements. The S and K emissions in Seoul were associated with many different sources, including coal burning, industrial activities, biomass burning, and vehicular activity (Table 2, PCA). In contrast, in Seosan, S and K were mainly associated with coal combustion and biomass burning (Table 2, PCA). At both locations, exposure to Si was primarily due to crustal sources.

3.5.2. Non-Carcinogenic Health Risks

The non-carcinogenic potential health risks due to elements (Pb, Cr, Cu, V, Mn, Ni, Zn, and As) through various exposure pathways (i.e., dermal contact, ingestion, and inhalation) at the Seoul and Seosan sites were estimated via the HQ (Table 4). In Seoul, the HQ values for adults were 1.6×10^{-5}, 8.5×10^{-5}, and 3.2×10^{-12}, while those for children were 1.5×10^{-4}, 3.3×10^{-4}, and 7.4×10^{-12}, through ingestion, dermal, and inhalation contact, respectively. In Seosan, the HQ values for adults were 1.4×10^{-5}, 8.4×10^{-5}, and 3.8×10^{-12}, while those for children were 1.3×10^{-4}, 3.3×10^{-4}, and 8.8×10^{-12}, through ingestion, dermal contact, and inhalation, respectively. At both sites, the HQ values associated with As, Cr, Pb, Ni Cu, Zn, and Mn were primarily attributed to dermal contact in adults (8.46×10^{-5}) and children (3.35×10^{-4}). Moreover, at both sites, the dermal exposure to Cr had the highest estimated HQ values for both adults (3.67×10^{-5}) and children (1.45×10^{-4}) (Table 4). The estimated HQ values were higher for children than for adults at both locations for all exposure routes (Table 4).

Table 4. Hazard quotient (HQ) and hazard index (HI) of components in $PM_{2.5}$ via ingestion (HQing), dermal (HQder), and inhalation (HQinh) for adults and children in rural and urban areas in South Korea during the winter.

Element	Adult			Children		
	HQing	HQder	HQinh	HQing	HQder	HQinh
Seoul						
Cr	2.8×10^{-07}	3.7×10^{-05}	1.3×10^{-13}	2.6×10^{-06}	1.5×10^{-04}	3.1×10^{-13}
Mn	2.0×10^{-07}	8.3×10^{-06}	3.0×10^{-12}	1.9×10^{-06}	3.3×10^{-05}	6.9×10^{-12}
Ni	1.7×10^{-08}	1.1×10^{-07}	7.7×10^{-17}	1.6×10^{-07}	4.2×10^{-07}	1.8×10^{-16}
Cu	7.8×10^{-08}	1.7×10^{-08}	3.6×10^{-16}	7.3×10^{-07}	6.8×10^{-08}	8.4×10^{-16}
V	6.1×10^{-08}	1.6×10^{-05}	2.8×10^{-16}	5.7×10^{-07}	6.2×10^{-05}	6.6×10^{-16}
Zn	1.2×10^{-07}	3.8×10^{-08}	5.3×10^{-16}	1.1×10^{-06}	1.5×10^{-07}	1.2×10^{-15}
As	1.1×10^{-05}	5.3×10^{-06}	5.0×10^{-14}	1.0×10^{-04}	2.1×10^{-05}	1.2×10^{-13}
Pb	4.2×10^{-06}	1.9×10^{-05}	1.9×10^{-14}	3.9×10^{-05}	7.4×10^{-05}	4.5×10^{-14}
HQ	1.6×10^{-05}	8.5×10^{-05}	3.2×10^{-12}	1.5×10^{-04}	3.3×10^{-04}	7.4×10^{-12}
HI = ΣHQ		1.0×10^{-04}			4.8×10^{-04}	
Seosan						
Cr	2.8×10^{-07}	3.8×10^{-05}	1.4×10^{-13}	2.7×10^{-06}	1.5×10^{-04}	3.2×10^{-13}
Mn	2.4×10^{-07}	1.0×10^{-05}	3.6×10^{-12}	2.3×10^{-06}	4.0×10^{-05}	8.3×10^{-12}
Ni	2.5×10^{-08}	1.5×10^{-07}	1.1×10^{-16}	2.3×10^{-07}	6.0×10^{-07}	2.6×10^{-16}
Cu	7.2×10^{-08}	1.6×10^{-08}	3.3×10^{-16}	6.8×10^{-07}	6.3×10^{-08}	7.7×10^{-16}
V	5.1×10^{-08}	1.3×10^{-05}	2.4×10^{-16}	4.8×10^{-07}	5.2×10^{-05}	5.5×10^{-16}
Zn	1.2×10^{-07}	3.9×10^{-08}	5.5×10^{-16}	1.1×10^{-06}	1.6×10^{-07}	1.3×10^{-15}
As	9.0×10^{-06}	4.4×10^{-06}	4.1×10^{-14}	8.4×10^{-05}	1.7×10^{-05}	9.6×10^{-14}
Pb	4.2×10^{-06}	1.9×10^{-05}	1.9×10^{-14}	3.9×10^{-05}	7.4×10^{-05}	4.5×10^{-14}
HQ	1.4×10^{-05}	8.4×10^{-05}	3.8×10^{-12}	1.3×10^{-04}	3.3×10^{-04}	8.8×10^{-12}
HI = ΣHQ		9.8×10^{-05}			4.6×10^{-04}	

The estimated HI was higher in Seoul than in Seosan for adults and children (Table 4). In Seoul and Seosan, the HI was higher for children (4.8×10^{-4} and 4.6×10^{-4}, respectively) than for adults (1.0×10^{-4} and 9.8×10^{-5}, respectively). One-way ANOVA with Tukey's test and paired *t*-tests was used to assess the statistical differences in HI between Seoul and Seosan (Tables S4 and S5). The HIs of the elements at the Seoul and Seosan sites did not reveal any significant differences ($p > 0.05$). Furthermore, the exposures to $PM_{2.5}$-bound trace elements were not significantly different between Seoul and Seosan ($p > 0.05$). The HI was within the permissible limit (HI < 1) at both sites, indicating no potential non-carcinogenic health risks to humans. According to a previous study conducted in the Chinese province of Shandong, the health risks from As and Zn primarily occurred via

dermal contact and ingestion [60]. Adults were more likely to be harmed by dermal contact, whereas children were more likely to be harmed by ingestion [115].

3.5.3. Carcinogenic Risk

In Seoul and Seosan, the potential CRs of As, Ni, Cr, and Pb were estimated for inhalation, ingestion, and dermal contact (Figure 4). In Seoul, for both adults and children, the CR values were higher for ingestion (3.2×10^{-9} and 7.5×10^{-9}, respectively) than for dermal contact (1.5×10^{-9} and 1.4×10^{-9}, respectively) and inhalation (4.2×10^{-18} and 2.4×10^{-18}, respectively). At Seosan, for both adults and children, the CR values were also higher for ingestion (3.0×10^{-9} and 6.9×10^{-9}, respectively) than for dermal contact (1.47×10^{-9} and 1.46×10^{-9}, respectively) and inhalation (5.0×10^{-18} and 2.9×10^{-18}, respectively). Furthermore, throughout the research period, the CR values for Cr, Ni, As, and Pb via all exposure routes were higher in Seoul than in Seosan. In Seoul, the highest CR value was for As ingestion by children (CR, 3.9×10^{-9}), whereas the highest CR value in Seosan was for Pb ingestion by children (CR, 3.32×10^{-9}). The CR values for Cr, As, Ni, and Pb in PM$_{2.5}$ at both sites were less than 1×10^{-6} for adults and children for all exposure routes; therefore, the risk of developing cancer from these toxic elements would be considered acceptable under most regulatory programs (Figure 4). According to a study conducted in rural and urban areas of northern Zhejiang Province, China, PM$_{2.5}$-bound elements posed significant non-CRs and CRs to the general public [10].
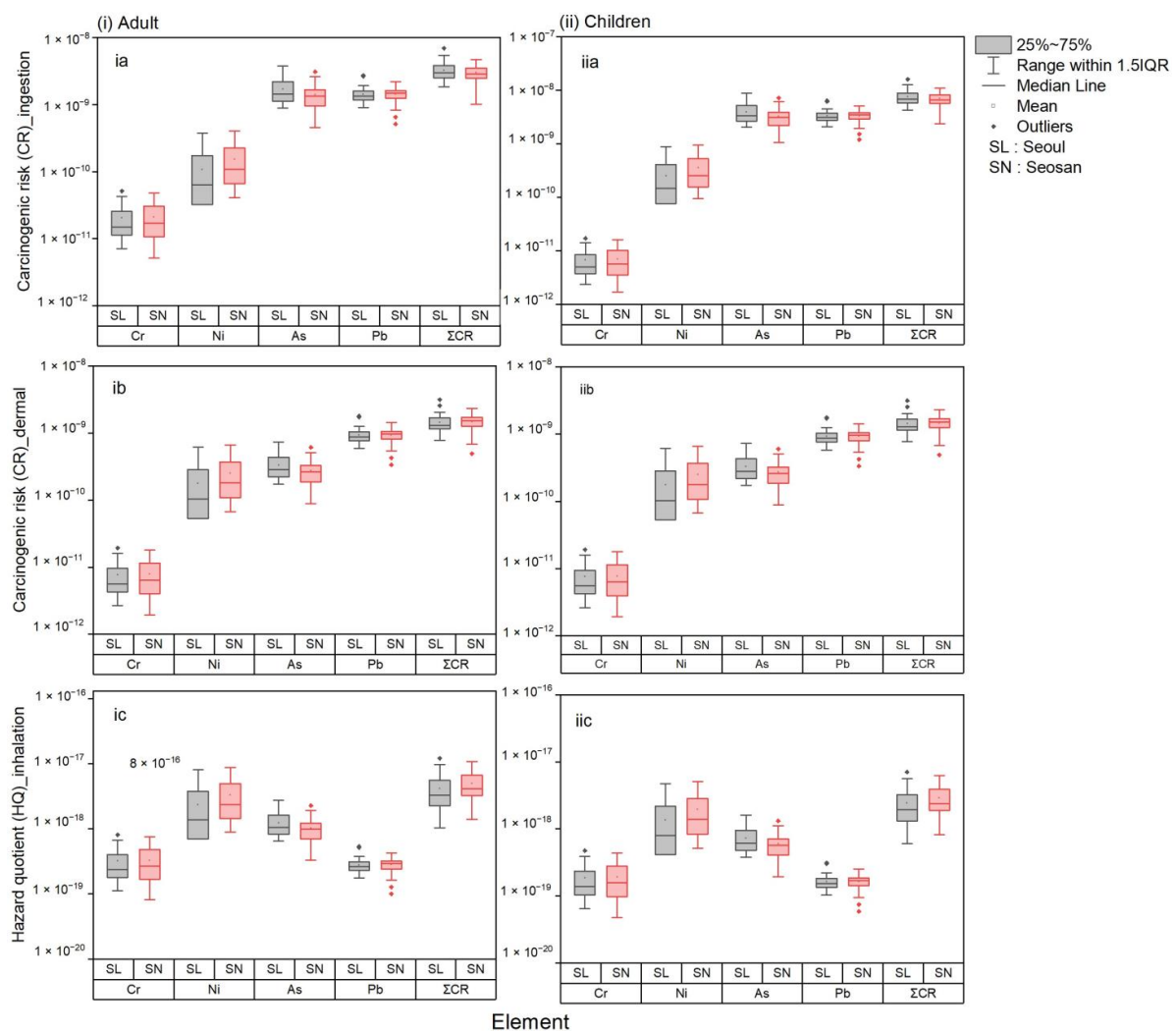
Figure 4. Cancer risk (CR) associated with elements in PM$_{2.5}$ in Seoul and Seosan during the winter of 2020–2021.

4. Conclusions

In this study, the trace constituents of $PM_{2.5}$ in Seoul and Seosan, South Korea, were measured during winter. The most abundant elements at the study sites were S and crustal elements (Si, Ca, Fe, and Ti). Additionally, the morning element concentrations were higher than the afternoon and evening element concentrations, which could be attributed to high traffic volumes and favorable weather conditions (lower T, lower WS, and higher RH). $PM_{2.5}$ concentrations were higher than 35 μg m^{-3} during episodic events, primarily due to high concentrations of S, K, and crustal elements at both study sites. Most elements exhibited spatial variation in their average concentration. For example, S was higher in Seoul, whereas crustal elements were higher in Seosan. The DDFs of the crustal elements (Si, Fe, and Ca) were greater than the DDFs of the primarily anthropogenic elements (Cu, Ni, Pb, Zn, Cr) in both Seoul and Seosan. During the winter, children were exposed to more elements by ingestion, dermal contact, and inhalation than adults in Seoul and Seosan. The health risk assessment for element exposure suggested no significant carcinogenic or non-carcinogenic effects in children and adults for either of the study sites. Compared with other elements, As and Pb were found to have higher CR values for adults and children at both study sites. In Seoul, higher CR levels were mostly linked to anthropogenic sources (traffic emissions, coal combustion, and biomass burning), whereas in Seosan they were linked to coal and biomass burning. We also suggest that future scientists and policymakers use these trace element concentration and health risk estimation results with caution, because they are specific to Seoul and Seosan.

Supplementary Materials: The following supporting information can be downloaded at: https://www.mdpi.com/article/10.3390/atmos14040753/s1, Text S1: Temporal variation of $PM_{2.5}$; Text S2: Estimation of the origins of the elements [113,114]; Table S1: Method detection limits (ng m^{-3}) of trace elements analyzed using Xact 605i; Table S2: Values to be used as guidelines for estimating the health risks posed by $PM_{2.5}$-bound trace elements via various pathways [115–118]; Table S3: Comparison of $PM_{2.5}$ (μg/m^3) and trace element (ng m^{-3}) concentrations at the study sites with those from other studies [11,28,38,41,60,106,119]; Table S4: One-way ANOVA with Tukey's test and paired *t*-tests of daily mean $PM_{2.5}$ and chemical species concentrations in Seoul and Seosan; Table S5: One-way ANOVA with Tukey's test and paired *t*-tests of health and exposure associated with $PM_{2.5}$-bound trace elements in Seoul and Seosan; Figure S1: Study sites in South Korea; Figure S2: Daily variation of minor elements in Seoul and Seosan during the winter period; Figure S3: Fire spots in South Korea and neighboring countries during the sampling period. Image retrieved from NASA's FIRMS VIIRS satellite (https://firms.modaps.eosdis.nasa.gov/ accessed on 2 April 2023.); Figure S4: $PM_{2.5}$-bound element exposure assessment over the Seoul (grey box) and Seosan (red box) locations in South Korea during the winter of 2020–2021. The values in this figure show TE exposure assessment based on daily average concentrations. Ingestion: chemical daily intake (CDI), dermal contact: dermal absorbed dose (DAD), and inhalation: exposure concentration (EC) were used to estimate exposure to elements in $PM_{2.5}$.

Author Contributions: Conceptualization, K.L.; Methodology, K.L. and J.N.; Investigation, J.N.; Data curation, J.N. and J.A.; Writing—original draft, J.N.; Writing—review and editing, K.L., J.N. and M.S.; Visualization, J.N.; Supervision, M.S.; Project administration, J.L. and M.S. All authors have read and agreed to the published version of the manuscript.

Institutional Review Board Statement: Not applicable.

Informed Consent Statement: Not applicable.

Data Availability Statement: Data will be made available upon reasonable request.

Conflicts of Interest: The authors declare that they have no known competing financial interests or personal relationships that could have appeared to influence the work reported in this paper.

References

1. Cao, J.J.; Wang, Q.Y.; Chow, J.C.; Watson, J.G.; Tie, X.X.; Shen, Z.X.; Wang, P.; An, Z.S. Impacts of Aerosol Compositions on Visibility Impairment in Xi'an, China. *Atmos. Environ.* **2012**, *59*, 559–566. [CrossRef]
2. Akhbarizadeh, R.; Dobaradaran, S.; Amouei Torkmahalleh, M.; Saeedi, R.; Aibaghi, R.; Faraji Ghasemi, F. Suspended Fine Particulate Matter (PM2.5), Microplastics (MPs), and Polycyclic Aromatic Hydrocarbons (PAHs) in Air: Their Possible Relationships and Health Implications. *Environ. Res.* **2021**, *192*, 110339. [CrossRef] [PubMed]
3. Cohen, A.J.; Brauer, M.; Burnett, R.; Anderson, H.R.; Frostad, J.; Estep, K.; Balakrishnan, K.; Brunekreef, B.; Dandona, L.; Dandona, R.; et al. Estimates and 25-Year Trends of the Global Burden of Disease Attributable to Ambient Air Pollution: An Analysis of Data from the Global Burden of Diseases Study 2015. *Lancet* **2017**, *389*, 1907–1918. [CrossRef] [PubMed]
4. Gu, H.; Yan, W.; Elahi, E.; Cao, Y. Air Pollution Risks Human Mental Health: An Implication of Two-Stages Least Squares Estimation of Interaction Effects. *Environ. Sci. Pollut. Res.* **2020**, *27*, 2036–2043. [CrossRef]
5. Kioumourtzoglou, M.-A.; Spiegelman, D.; Szpiro, A.A.; Sheppard, L.; Kaufman, J.D.; Yanosky, J.D.; Williams, R.; Laden, F.; Hong, B.; Suh, H. Exposure Measurement Error in PM2.5 Health Effects Studies: A Pooled Analysis of Eight Personal Exposure Validation Studies. *Environ. Health A Glob. Access Sci. Source* **2014**, *13*, 1–11. [CrossRef]
6. Lippmann, M. Toxicological and Epidemiological Studies of Cardiovascular Effects of Ambient Air Fine Particulate Matter (PM2.5) and Its Chemical Components: Coherence and Public Health Implications. *Crit. Rev. Toxicol.* **2014**, *44*, 299–347. [CrossRef] [PubMed]
7. Zheng, Y.; Wen, X.; Bian, J.; Lipkind, H.; Hu, H. Associations between the Chemical Composition of PM2.5 and Gestational Diabetes Mellitus. *Environ. Res.* **2021**, *198*, 110470. [CrossRef]
8. Jo, Y.S.; Lim, M.N.; Han, Y.J.; Kim, W.J. Epidemiological Study of PM2.5 and Risk of COPD-Related Hospital Visits in Association with Particle Constituents in Chuncheon, Korea. *Int. J. COPD* **2018**, *13*, 299–307. [CrossRef]
9. Jin, Q.; Gong, L.; Liu, S.; Ren, R. Assessment of Trace Elements Characteristics and Human Health Risk of Exposure to Ambient PM2.5 in Hangzhou, China. *Int. J. Environ. Anal. Chem.* **2017**, *97*, 983–1002. [CrossRef]
10. Xu, J.; Jia, C.; Yu, H.; Xu, H.; Ji, D.; Wang, C.; Xiao, H.; He, J. Characteristics, Sources, and Health Risks of PM2.5-Bound Trace Elements in Representative Areas of Northern Zhejiang Province, China. *Chemosphere* **2021**, *272*, 129632. [CrossRef]
11. Zhang, J.; Zhou, X.; Wang, Z.; Yang, L.; Wang, J.; Wang, W. Science of the Total Environment Trace Elements in PM 2.5 in Shandong Province: Source Identification and Health Risk Assessment. *Sci. Total Environ.* **2018**, *621*, 558–577. [CrossRef]
12. Li, Y.; Zhang, Z.; Liu, H.; Zhou, H.; Fan, Z.; Lin, M.; Wu, D.; Xia, B. Characteristics, Sources and Health Risk Assessment of Toxic Heavy Metals in PM2.5 at a Megacity of Southwest China. *Environ. Geochem. Health* **2016**, *38*, 353–362. [CrossRef] [PubMed]
13. Park, S.K.; Adar, S.D.; O'Neill, M.S.; Auchincloss, A.H.; Szpiro, A.; Bertoni, A.G.; Navas-Acien, A.; Kaufman, J.D.; Diez-Roux, A.V. Long-Term Exposure to Air Pollution and Type 2 Diabetes Mellitus in a Multiethnic Cohort. *Am. J. Epidemiol.* **2015**, *181*, 327–336. [CrossRef] [PubMed]
14. Moufarrej, L.; Verdin, A.; Cazier, F.; Ledoux, F.; Courcot, D. Oxidative Stress Response in Pulmonary Cells Exposed to Different Fractions of PM2.5-0.3 from Urban, Traffic and Industrial Sites. *Environ. Res.* **2023**, *216*, 114572. [CrossRef]
15. Tao, Y.; Kou, L.; Chai, Y.; Kwan, M.P. Associations of Co-Exposures to Air Pollution and Noise with Psychological Stress in Space and Time: A Case Study in Beijing, China. *Environ. Res.* **2021**, *196*, 110399. [CrossRef]
16. Gorai, A.K.; Tchounwou, P.B.; Biswal, S.S.; Tuluri, F. Spatio-Temporal Variation of Particulate Matter(PM2.5) Concentrations and Its Health Impacts in a Mega City, Delhi in India. *Environ. Health Insights* **2018**, *12*, 1178630218792861. [CrossRef]
17. Bae, M.S.; Demerjian, K.L.; Schwab, J.J. Seasonal Estimation of Organic Mass to Organic Carbon in PM2.5 at Rural and Urban Locations in New York State. *Atmos. Environ.* **2006**, *40*, 7467–7479. [CrossRef]
18. Balasubramanian, R.; Qian, W.B.; Decesari, S.; Facchini, M.C.; Fuzzi, S. Comprehensive Characterization of PM2.5 Aerosols in Singapore. *J. Geophys. Res. Atmos.* **2003**, *108*, D16. [CrossRef]
19. Park, S.M.; Song, I.H.; Park, J.S.; Oh, J.; Moon, K.J.; Shin, H.J.; Ahn, J.Y.; Lee, M.-D.; Kim, J.; Lee, G. Variation of PM2.5 Chemical Compositions and Their Contributions to Light Extinction in Seoul. *Aerosol Air Qual. Res.* **2018**, *18*, 2220–2229. [CrossRef]
20. Lu, X.; Zhang, X.; Li, L.Y.; Chen, H. Assessment of Metals Pollution and Health Risk in Dust from Nursery Schools in Xi'an, China. *Environ. Res.* **2014**, *128*, 27–34. [CrossRef]

21. Sánchez-Soberón, F.; Rovira, J.; Sierra, J.; Mari, M.; Domingo, J.L.; Schuhmacher, M. Seasonal Characterization and Dosimetry-Assisted Risk Assessment of Indoor Particulate Matter (PM10-2.5, PM2.5-0.25, and PM0.25) Collected in Different Schools. *Environ. Res.* **2019**, *175*, 287–296. [CrossRef] [PubMed]

22. Natsagdorj, A.; Tugsbayan, B.; Battumur, T.; Oyuntsetseg, B.; Lee, J.; Kim, Y.P.; Usuhbayar, B. Seasonal Concentrations of Elements in Both Indoor and Outdoor Housing in PM2.5. *WIT Trans. Ecol. Environ.* **2021**, *252*, 53–65. [CrossRef]

23. Anand, A.; Yadav, S.; Phuleria, H.C. Chemical Characteristics and Oxidative Potential of Indoor and Outdoor PM2.5 in Densely Populated Urban Slums. *Environ. Res.* **2022**, *212*, 113562. [CrossRef] [PubMed]

24. Nirmalkar, J.; Haswani, D.; Singh, A.; Kumar, S.; Sunder Raman, R. Concentrations, Transport Characteristics, and Health Risks of PM2.5-Bound Trace Elements over a National Park in Central India. *J. Environ. Manag.* **2021**, *293*, 112904. [CrossRef]

25. Aggarwal, S.G.; Kumar, S.; Mandal, P.; Sarangi, B.; Singh, K.; Pokhariyal, J.; Mishra, S.K.; Agarwal, S.; Sinha, D.; Singh, S.; et al. Traceability Issue in PM2.5 and PM10 Measurements. *Mapan—J. Metrol. Soc. India* **2013**, *28*, 153–166. [CrossRef]

26. Xia, L.; Gao, Y. Characterization of Trace Elements in PM2.5 Aerosols in the Vicinity of Highways in Northeast New Jersey in the U.S. East Coast. *Atmos. Pollut. Res.* **2011**, *2*, 34–44. [CrossRef]

27. Li, Y.; Chang, M.; Ding, S.; Wang, S.; Ni, D.; Hu, H. Monitoring and Source Apportionment of Trace Elements in PM2.5: Implications for Local Air Quality Management. *J. Environ. Manag.* **2017**, *196*, 16–25. [CrossRef]

28. Hao, Y.; Meng, X.; Yu, X.; Lei, M.; Li, W.; Shi, F.; Yang, W.; Zhang, S.; Xie, S. Characteristics of Trace Elements in PM2.5 and PM10 of Chifeng, Northeast China: Insights into Spatiotemporal Variations and Sources. *Atmos. Res.* **2018**, *213*, 550–561. [CrossRef]

29. Tsai, Y.I.; Sopajaree, K.; Kuo, S.C.; Yu, S.P. Potential PM2.5 Impacts of Festival-Related Burning and Other Inputs on Air Quality in an Urban Area of Southern Taiwan. *Sci. Total Environ.* **2015**, *527–528*, 65–79. [CrossRef]

30. Reff, A.; Bhave, P.V.; Simon, H.; Pace, T.G.; Pouliot, G.A.; Mobley, J.D.; Houyoux, M. Emissions Inventory of PM2.5 Trace Elements across the United States. *Environ. Sci. Technol.* **2009**, *43*, 5790–5796. [CrossRef]

31. Baensch-Baltruschat, B.; Kocher, B.; Stock, F.; Reifferscheid, G. Tyre and Road Wear Particles (TRWP)—A Review of Generation, Properties, Emissions, Human Health Risk, Ecotoxicity, and Fate in the Environment. *Sci. Total Environ.* **2020**, *733*, 137823. [CrossRef] [PubMed]

32. Tchounwou, P.B.; Yedjou, C.G.; Patlolla, A.K.; Sutton, D.J. *Molecular, Clinical and Environmental Toxicicology Volume 3: Environmental Toxicology*; Springer: Berlin/Heidelberg, Germany, 2012; Volume 101, ISBN 978-3-7643-8339-8.

33. Alavanja, M.; Baron, J.A.; Brownson, R.C.; Buffler, P.A.; DeMarini, D.M.; Djordjevic, M.V.; Doll, R.; Fontham, E.T.H.; Gao, Y.T.; Gray, N.; et al. Tobacco Smoke and Involuntary Smoking. *IARC Monogr. Eval. Carcinog. Risks Hum.* **2004**, *83*, 1–1413.

34. Mulware, S.J. Trace Elements and Carcinogenicity: A Subject in Review. *3 Biotech* **2013**, *3*, 85–96. [CrossRef] [PubMed]

35. Domingo, J.L.; Nadal, M. Domestic Waste Composting Facilities: A Review of Human Health Risks. *Environ. Int.* **2009**, *35*, 382–389. [CrossRef]

36. Kioumourtzoglou, M.A.; Schwartz, J.D.; Weisskopf, M.G.; Melly, S.J.; Wang, Y.; Dominici, F.; Zanobetti, A. Long-Term PM2.5 Exposure and Neurological Hospital Admissions in the Northeastern United States. *Environ. Health Perspect.* **2016**, *124*, 23–29. [CrossRef]

37. Dockery, D.W. Health Effects of Particulate Air Pollution. *Ann. Epidemiol.* **2009**, *19*, 257–263. [CrossRef]

38. Liu, L.; Liu, Y.; Wen, W.; Liang, L.; Ma, X.; Jiao, J.; Guo, K. Source Identification of Trace Elements in PM2.5 at a Rural Site in the North China Plain. *Atmosphere* **2020**, *11*, 179. [CrossRef]

39. Kang, C.M.; Sunwoo, Y.; Lee, H.S.; Kang, B.W.; Lee, S.K. Atmospheric Concentrations of PM2.5 Trace Elements in the Seoul Urban Area of South Korea. *J. Air Waste Manag. Assoc.* **2004**, *54*, 432–439. [CrossRef]

40. Lee, S.; Han, C.; Ahn, J.; Han, Y.; Lee, A.-h.; Ro, S.; Hong, S. Characterization of Trace Elements and Pb Isotopes in PM2.5 and Isotopic Source Identification during Haze Episodes in Seoul, Korea. *Atmos. Pollut. Res.* **2022**, *13*, 101442. [CrossRef]

41. Won, S.R.; Shim, I.K.; Kim, J.; Ah Ji, H.; Lee, Y.; Lee, J.; Ghim, Y.S. Pm2.5 and Trace Elements in Underground Shopping Districts in the Seoul Metropolitan Area, Korea. *Int. J. Environ. Res. Public Health* **2021**, *18*, 297. [CrossRef] [PubMed]

42. Kim, N.K.; Kim, Y.P.; Ghim, Y.S.; Song, M.J.; Kim, C.H.; Jang, K.S.; Lee, K.Y.; Shin, H.J.; Jung, J.S.; Wu, Z.; et al. Spatial Distribution of PM2.5 Chemical Components during Winter at Five Sites in Northeast Asia: High Temporal Resolution Measurement Study. *Atmos. Environ.* **2022**, *290*, 119359. [CrossRef]

43. Choi, N.R.; Park, S.; Ju, S.; Lim, Y.-B.; Lee, J.Y.; Kim, E.; Kim, S.; Shin, H.J.; Kim, Y.P. Contribution of Liquid Water Content Enhancing Aqueous Phase Reaction Forming Ambient Particulate Nitrosamines. *Environ. Pollut.* **2022**, *303*, 119142. [CrossRef] [PubMed]

44. Rhee, K.A.; Kim, J.K.; Lee, Y.I.; Ulfarsson, G.F. Spatial Regression Analysis of Traffic Crashes in Seoul. *Accid. Anal. Prev.* **2016**, *91*, 190–199. [CrossRef] [PubMed]

45. Park, S.; Son, S.C.; Lee, K.Y. Chemical Characteristics of PM2.5 during Spring and Fall at Two Sites in Chungcheongnam-Do, South Korea; Insight into Fe Solubility and SO42− Formation. *Atmos. Pollut. Res.* **2022**, *13*, 101350. [CrossRef]

46. Services, C.E. Xact ®625i Multi-Metals Monitoring System. Available online: https://www.ecotech.com/wp-content/uploads/2017/03/Cooper-Environmental-Monitoring-625i-Spec-Sheet.pdf (accessed on 2 April 2023).

47. Rai, P.; Furger, M.; Slowik, J.G.; Canonaco, F.; Fröhlich, R.; Hüglin, C.; Minguillón, M.C.; Petterson, K.; Baltensperger, U.; Prévôt, A.S.H. Source Apportionment of Highly Time-Resolved Elements during a Firework Episode from a Rural Freeway Site in Switzerland. *Atmos. Chem. Phys.* **2020**, *20*, 1657–1674. [CrossRef]

48. Bhowmik, H.S.; Shukla, A.; Lalchandani, V.; Dave, J.; Rastogi, N.; Kumar, M.; Singh, V.; Tripathi, S.N. Inter-Comparison of Online and Offline Methods for Measuring Ambient Heavy and Trace Elements and Water-Soluble Inorganic Ions (NO3-, SO42-, NH4+, and Cl-) in PM2.5over a Heavily Polluted Megacity, Delhi. *Atmos. Meas. Technol.* **2022**, *15*, 2667–2684. [CrossRef]

49. Furger, M.; Rai, P.; Slowik, J.G.; Cao, J.; Visser, S.; Baltensperger, U.; Prévôt, A.S.H. Automated Alternating Sampling of PM10 and PM2.5 with an Online XRF Spectrometer. *Atmos. Environ. X* **2020**, *5*, 100065. [CrossRef]

50. Mariraj Mohan, S. An Overview of Particulate Dry Deposition: Measuring Methods, Deposition Velocity and Controlling Factors. *Int. J. Environ. Sci. Technol.* **2016**, *13*, 387–402. [CrossRef]

51. Chen, Y.; Paytan, A.; Chase, Z.; Measures, C.; Beck, A.J.; Sañudo-Wilhelmy, S.A.; Post, A.F. Sources and Fluxes of Atmospheric Trace Elements to the Gulf of Aqaba, Red Sea. *J. Geophys. Res. Atmos.* **2008**, *113*, 1–13. [CrossRef]

52. Gao, Y.; Nelson, E.D.; Field, M.P.; Ding, Q.; Li, H.; Sherrell, R.M.; Gigliotti, C.L.; Van Ry, D.A.; Glenn, T.R.; Eisenreich, S.J. Characterization of Atmospheric Trace Elements on PM2.5 Particulate Matter over the New York-New Jersey Harbor Estuary. *Atmos. Environ.* **2002**, *36*, 1077–1086. [CrossRef]

53. Hsu, S.C.; Wong, G.T.F.; Gong, G.C.; Shiah, F.K.; Huang, Y.T.; Kao, S.J.; Tsai, F.; Candice Lung, S.C.; Lin, F.J.; Lin, I.I.; et al. Sources, Solubility, and Dry Deposition of Aerosol Trace Elements over the East China Sea. *Mar. Chem.* **2010**, *120*, 116–127. [CrossRef]

54. Lu, R.; Turco, R.P.; Stolzenbach, K.; Friedlander, S.K.; Xiong, C.; Schiff, K.; Tiefenthaler, L.; Wang, G. Dry Deposition of Airborne Trace Metals on the Los Angeles Basin and Adjacent Coastal Waters. *J. Geophys. Res. Atmos.* **2003**, *108*, D2. [CrossRef]

55. Cao, S.; Duan, X.; Zhao, X.; Wang, B.; Ma, J.; Fan, D.; Sun, C.; He, B.; Wei, F.; Jiang, G. Health Risk Assessment of Various Metal(Loid)s via Multiple Exposure Pathways on Children Living near a Typical Lead-Acid Battery Plant, China. *Environ. Pollut.* **2015**, *200*, 16–23. [CrossRef]

56. Zheng, N.; Liu, J.; Wang, Q.; Liang, Z. Health Risk Assessment of Heavy Metal Exposure to Street Dust in the Zinc Smelting District, Northeast of China. *Sci. Total Environ.* **2010**, *408*, 726–733. [CrossRef]

57. Hu, Y.; Odman, M.T.; Chang, M.E.; Jackson, W.; Lee, S.; Edgerton, E.S.; Baumann, K.; Russell, A.G. Simulation of Air Quality Impacts from Prescribed Fires on an Urban Area. *Environ. Sci. Technol.* **2008**, *42*, 3676–3682. [CrossRef] [PubMed]

58. *US Environmental Protection Agency Exposure Factors Handbook: 2011 Edition*; U.S. Environmental Protection Agency: Philadelphia, PA, USA, 2011; pp. 1–1466.

59. Guo, F.; Tang, M.; Wang, X.; Yu, Z.; Wei, F.; Zhang, X.; Jin, M.; Wang, J.; Xu, D.; Chen, Z.; et al. Characteristics, Sources, and Health Risks of Trace Metals in PM2.5. *Atmos. Environ.* **2022**, *289*, 119314. [CrossRef]

60. Hu, X.; Zhang, Y.; Ding, Z.; Wang, T.; Lian, H.; Sun, Y.; Wu, J. Bioaccessibility and Health Risk of Arsenic and Heavy Metals (Cd, Co, Cr, Cu, Ni, Pb, Zn and Mn) in TSP and PM2.5 in Nanjing, China. *Atmos. Environ.* **2012**, *57*, 146–152. [CrossRef]

61. Kogianni, E.; Kouras, A.; Samara, C. Indoor Concentrations of PM2.5 and Associated Water-Soluble and Labile Heavy Metal Fractions in Workplaces: Implications for Inhalation Health Risk Assessment. *Environ. Sci. Pollut. Res.* **2021**, *28*, 58983–58993. [CrossRef] [PubMed]

62. EPA. *Risk Assessment Guidance for Superfund. Volume I Human Health Evaluation Manual (Part A)*; Environmental Protection Agency (EPA): Washington, DC, USA, 1989; Volume I, p. 289.

63. Lee, S.J.; Lee, H.Y.; Kim, S.J.; Kang, H.J.; Kim, H.; Seo, Y.K.; Shin, H.J.; Ghim, Y.S.; Song, C.K.; Choi, S.D. Pollution Characteristics of PM2.5 during High Concentration Periods in Summer and Winter in Ulsan, the Largest Industrial City in South Korea. *Atmos. Environ.* **2023**, *292*, 119418. [CrossRef]

64. Yuan, C.S.; Wong, K.W.; Tseng, Y.L.; Ceng, J.H.; Lee, C.E.; Lin, C. Chemical Significance and Source Apportionment of Fine Particles (PM2.5) in an Industrial Port Area in East Asia. *Atmos. Pollut. Res.* **2022**, *13*, 101349. [CrossRef]

65. Zhang, X.; Eto, Y.; Aikawa, M. Risk Assessment and Management of PM2.5-Bound Heavy Metals in the Urban Area of Kitakyushu, Japan. *Sci. Total Environ.* **2021**, *795*, 148748. [CrossRef]

66. Wedepohl, K.H. The Composition of the Continental Crust. *Int. Geophys.* **1986**, *34*, 213–241. [CrossRef]

67. Choi, J.-k.; Heo, J.B.; Ban, S.J.; Yi, S.M.; Zoh, K.D. Source Apportionment of PM2.5 at the Coastal Area in Korea. *Sci. Total Environ.* **2013**, *447*, 370–380. [CrossRef] [PubMed]

68. Park, J.; Ryoo, J.; Jee, J.; Song, M. Origins and Distributions of Atmospheric Ammonia in Jeonju during 2019~2020. *J. Korean Soc. Atmos. Environ.* **2020**, *36*, 262–274. [CrossRef]

69. De La Cruz, A.H.; Roca, Y.B.; Suarez-Salas, L.; Pomalaya, J.; Tolentino, D.A.; Gioda, A. Chemical Characterization of PM 2.5 at Rural and Urban Sites around the Metropolitan Area of Huancayo (Central Andes of Peru). *Atmosphere* **2019**, *10*, 21. [CrossRef]

70. Sawyer, S.F. Analysis of Variance: The Fundamental Concepts. *J. Man. Manip. Ther.* **2009**, *17*, 27E–38E. [CrossRef]

71. Kim, Y.; Lee, I.; Farquhar, J.; Kang, J.; Villa, I.M.; Kim, H. Multi Isotope Systematics of Precipitation to Trace the Sources of Air Pollutants in Seoul, Korea. *Environ. Pollut.* **2021**, *286*, 117548. [CrossRef]

72. Ray, I.; Das, R.; Chua, S.L.; Wang, X. Seasonal Variation of Atmospheric Pb Sources in Singapore—Elemental and Lead Isotopic Compositions of PM10 as Source Tracer. *Chemosphere* **2022**, *307*, 136029. [CrossRef]

73. Ying, Q.; Feng, M.; Song, D.; Wu, L.; Hu, J.; Zhang, H.; Kleeman, M.J.; Li, X. Improve Regional Distribution and Source Apportionment of PM 2.5 Trace Elements in China Using Inventory-Observation Constrained Emission Factors. *Sci. Total Environ.* **2018**, *624*, 355–365. [CrossRef]

74. Kayee, J.; Bureekul, S.; Sompongchaiyakul, P.; Wang, X.; Das, R. Sources of Atmospheric Lead (Pb) after Quarter Century of Phasing out of Leaded Gasoline in Bangkok, Thailand. *Atmos. Environ.* **2021**, *253*, 118355. [CrossRef]

75. Das, R.; Bin Mohamed Mohtar, A.T.; Rakshit, D.; Shome, D.; Wang, X. Sources of Atmospheric Lead (Pb) in and around an Indian Megacity. *Atmos. Environ.* **2018**, *193*, 57–65. [CrossRef]
76. Wu, P.C.; Huang, K.F. Tracing Local Sources and Long-Range Transport of PM10 in Central Taiwan by Using Chemical Characteristics and Pb Isotope Ratios. *Sci. Rep.* **2021**, *11*, 1–15. [CrossRef]
77. Fakhri, N.; Fadel, M.; Öztürk, F.; Keleş, M.; Iakovides, M.; Pikridas, M.; Abdallah, C.; Karam, C.; Sciare, J.; Hayes, P.L.; et al. Comprehensive Chemical Characterization of PM2.5 in the Large East Mediterranean-Middle East City of Beirut, Lebanon. *J. Environ. Sci.* **2023**, *133*, 118–137. [CrossRef]
78. Schauer, J.J.; Majestic, B.J.; Sheesley, R.J.; Shafer, M.M.; Deminter, J.T.; Mieritz, M. HEI Health Review Committee Improved Source Apportionment and Speciation of Low-Volume Particulate Matter Samples. *Res. Rep. Health. Eff. Inst.* **2010**, *3–75*, 77–89.
79. Salameh, D.; Detournay, A.; Pey, J.; Pérez, N.; Liguori, F.; Saraga, D.; Bove, M.C.; Brotto, P.; Cassola, F.; Massabò, D.; et al. PM2.5 Chemical Composition in Five European Mediterranean Cities: A 1-Year Study. *Atmos. Res.* **2015**, *155*, 102–117. [CrossRef]
80. Mamoudou, I.; Zhang, F.; Chen, Q.; Wang, P.; Chen, Y. Characteristics of PM2.5 from Ship Emissions and Their Impacts on the Ambient Air: A Case Study in Yangshan Harbor, Shanghai. *Sci. Total Environ.* **2018**, *640–641*, 207–216. [CrossRef] [PubMed]
81. Luo, Y.; Liu, S.; Che, L.; Yu, Y. Analysis of Temporal Spatial Distribution Characteristics of PM2.5 Pollution and the Influential Meteorological Factors Using Big Data in Harbin, China. *J. Air Waste Manag. Assoc.* **2021**, *71*, 964–973. [CrossRef]
82. Yang, W.; Wang, G.; Bi, C. Analysis of Long-Range Transport Effects on PM2.5 during a Short Severe Haze in Beijing, China. *Aerosol Air Qual. Res.* **2017**, *17*, 1510–1522. [CrossRef]
83. Pathak, R.K.; Wang, T.; Wu, W.S. Nighttime Enhancement of PM2.5 Nitrate in Ammonia-Poor Atmospheric Conditions in Beijing and Shanghai: Plausible Contributions of Heterogeneous Hydrolysis of N2O5 and HNO3 Partitioning. *Atmos. Environ.* **2011**, *45*, 1183–1191. [CrossRef]
84. Chen, R.; Jia, B.; Tian, Y.; Feng, Y. Source-Specific Health Risk Assessment of PM2.5-Bound Heavy Metals Based on High Time-Resolved Measurement in a Chinese Megacity: Insights into Seasonal and Diurnal Variations. *Ecotoxicol. Environ. Saf.* **2021**, *216*, 112167. [CrossRef]
85. Hou, S.; Zheng, N.; Tang, L.; Ji, X.; Li, Y.; Hua, X. Pollution Characteristics, Sources, and Health Risk Assessment of Human Exposure to Cu, Zn, Cd and Pb Pollution in Urban Street Dust across China between 2009 and 2018. *Environ. Int.* **2019**, *128*, 430–437. [CrossRef]
86. Hong, N.; Guan, Y.; Yang, B.; Zhong, J.; Zhu, P.; Ok, Y.S.; Hou, D.; Tsang, D.C.W.; Guan, Y.; Liu, A. Quantitative Source Tracking of Heavy Metals Contained in Urban Road Deposited Sediments. *J. Hazard. Mater.* **2020**, *393*, 122362. [CrossRef]
87. Alexakis, D.E. Multielement Contamination of Land in the Margin of Highways. *Land* **2021**, *10*, 230. [CrossRef]
88. Park, J.; Kim, H.; Kim, Y.; Heo, J.; Kim, S.W.; Jeon, K.; Yi, S.M.; Hopke, P.K. Source Apportionment of PM2.5 in Seoul, South Korea and Beijing, China Using Dispersion Normalized PMF. *Sci. Total Environ.* **2022**, *833*, 155056. [CrossRef]
89. Park, M.-B.; Lee, T.J.; Lee, E.S.; Kim, D.S. Enhancing Source Identification of Hourly PM2.5 Data in Seoul Based on a Dataset Segmentation Scheme by Positive Matrix Factorization (PMF). *Atmos. Pollut. Res.* **2019**, *10*, 1042–1059. [CrossRef]
90. Charron, A.; Harrison, R.M. Matter on a Heavily Trafficked London Highway: Sources and Processes. *Environ. Sci. Technol.* **2005**, *39*, 7768–7776. [CrossRef] [PubMed]
91. Pancras, J.P.; Landis, M.S.; Norris, G.A.; Vedantham, R.; Dvonch, J.T. Source Apportionment of Ambient Fine Particulate Matter in Dearborn, Michigan, Using Hourly Resolved PM Chemical Composition Data. *Sci. Total Environ.* **2013**, *448*, 2–13. [CrossRef] [PubMed]
92. One, K.H.; Kim, J.; One, Y.K. A Study on the Factors Affecting the Air Environment in Chungnam Province—Focusing on Cheonan, Dangjin, and Seosan. *Am. J. Orthod. Dentofacial. Orthop.* **2021**, *22*, 118–127.
93. Huang, H.; Jiang, Y.; Xu, X.; Cao, X. In Vitro Bioaccessibility and Health Risk Assessment of Heavy Metals in Atmospheric Particulate Matters from Three Different Functional Areas of Shanghai, China. *Sci. Total Environ.* **2018**, *610–611*, 546–554. [CrossRef]
94. Ma, W.; Tai, L.; Qiao, Z.; Zhong, L.; Wang, Z.; Fu, K.; Chen, G. Contamination Source Apportionment and Health Risk Assessment of Heavy Metals in Soil around Municipal Solid Waste Incinerator: A Case Study in North China. *Sci. Total Environ.* **2018**, *631–632*, 348–357. [CrossRef]
95. Mainka, A.; Zajusz-Zubek, E.; Kaczmarek, K. PM2.5 in Urban and Rural Nursery Schools in Upper Silesia, Poland: Trace Elements Analysis. *Int. J. Environ. Res. Public Health* **2015**, *12*, 7990–8008. [CrossRef] [PubMed]
96. Makkonen, U.; Hellén, H.; Anttila, P.; Ferm, M. Size Distribution and Chemical Composition of Airborne Particles in South-Eastern Finland during Different Seasons and Wildfire Episodes in 2006. *Sci. Total Environ.* **2010**, *408*, 644–651. [CrossRef]
97. Sánchez De La Campa, A.M.; De La Rosa, J.; González-Castanedo, Y.; Fernández-Camacho, R.; Alastuey, A.; Querol, X.; Stein, A.F.; Ramos, J.L.; Rodríguez, S.; Orellana, I.G.; et al. Levels and Chemical Composition of PM in a City near a Large Cu-Smelter in Spain. *J. Environ. Monit.* **2011**, *13*, 1276–1287. [CrossRef]
98. Pant, P.; Harrison, R.M. Critical Review of Receptor Modelling for Particulate Matter: A Case Study of India. *Atmos. Environ.* **2012**, *49*, 1–12. [CrossRef]
99. Lee, J.H.; Yoshida, Y.; Turpin, B.J.; Hopke, P.K.; Poirot, R.L.; Lioy, P.J.; Oxley, J.C. Identification of Sources Contributing to Mid-Atlantic Regional Aerosol. *J. Air Waste Manag. Assoc.* **2002**, *52*, 1186–1205. [CrossRef]
100. Jain, S.; Sharma, S.K.; Vijayan, N.; Mandal, T.K. Seasonal Characteristics of Aerosols (PM2.5 and PM10) and Their Source Apportionment Using PMF: A Four Year Study over Delhi, India. *Environ. Pollut.* **2020**, *262*, 114337. [CrossRef] [PubMed]

101. Galindo, N.; Yubero, E.; Nicolás, J.F.; Crespo, J.; Varea, M.; Gil-Moltó, J. Regional and Long-Range Transport of Aerosols at Mt. Aitana, Southeastern Spain. *Sci. Total Environ.* **2017**, *584–585*, 723–730. [CrossRef] [PubMed]

102. Golley, J. Regional Patterns of Industrial Development during China's Economic Transition. *Econ. Transit.* **2002**, *10*, 761–801. [CrossRef]

103. Zhang, Y.; Liu, X.; Zhang, L.; Tang, A.; Goulding, K.; Collett, J.L. Evolution of Secondary Inorganic Aerosols amidst Improving PM2.5 Air Quality in the North China Plain. *Environ. Pollut.* **2021**, *281*, 117027. [CrossRef] [PubMed]

104. Liang, L.; Engling, G.; Cheng, Y.; Liu, X.; Du, Z.; Ma, Q.; Zhang, X.; Sun, J.; Xu, W.; Liu, C.; et al. Biomass Burning Impacts on Ambient Aerosol at a Background Site in East China: Insights from a Yearlong Study. *Atmos. Res.* **2020**, *231*, 104660. [CrossRef]

105. Li, X.; Chen, M.; Le, H.P.; Wang, F.; Guo, Z.; Iinuma, Y.; Chen, J.; Herrmann, H. Atmospheric Outflow of PM2.5 Saccharides from Megacity Shanghai to East China Sea: Impact of Biological and Biomass Burning Sources. *Atmos. Environ.* **2016**, *143*, 1–14. [CrossRef]

106. Duan, L.; Song, J.; Xu, Y.; Li, X.; Zhang, Y. The Distribution, Enrichment and Source of Potential Harmful Elements in Surface Sediments of Bohai Bay, North China. *J. Hazard. Mater.* **2010**, *183*, 155–164. [CrossRef]

107. Pan, Y.P.; Wang, Y.S. Atmospheric Wet and Dry Deposition of Trace Elements at 10 Sites in Northern China. *Atmos. Chem. Phys.* **2015**, *15*, 951–972. [CrossRef]

108. Yi, S.M.; Shahin, U.; Sivadechathep, J.; Sofuoglu, S.C.; Holsen, T.M. Overall Elemental Dry Deposition Velocities Measured around Lake Michigan. *Atmos. Environ.* **2001**, *35*, 1133–1140. [CrossRef]

109. Tasdemir, Y.; Kural, C.; Cindoruk, S.S.; Vardar, N. Assessment of Trace Element Concentrations and Their Estimated Dry Deposition Fluxes in an Urban Atmosphere. *Atmos. Res.* **2006**, *81*, 17–35. [CrossRef]

110. Jiang, Y.; Shi, L.; Guang, A.-l.; Mu, Z.; Zhan, H.; Wu, Y. Contamination Levels and Human Health Risk Assessment of Toxic Heavy Metals in Street Dust in an Industrial City in Northwest China. *Environ. Geochem. Health* **2018**, *40*, 2007–2020. [CrossRef] [PubMed]

111. Zhang, L.; He, J.; Gong, S.; Guo, X.; Zhao, T.; Zhou, C.; Wang, H.; Mo, J.; Gui, K.; Zheng, Y.; et al. Effect of Vegetation Seasonal Cycle Alterations to Aerosol Dry Deposition on PM2.5 Concentrations in China. *Sci. Total Environ.* **2022**, *828*, 154211. [CrossRef] [PubMed]

112. Qin, J.; Mbululo, Y.; Yang, M.; Yuan, Z.; Nyihirani, F.; Zheng, X. Chemical Composition and Deposition Fluxes of Water-Soluble Inorganic Ions on Dry and Wet Deposition Samples in Wuhan, China. *Int. J. Environ. Res. Public Health* **2019**, *16*, 132. [CrossRef]

113. Chen, F.; Zhang, X.; Zhu, X.; Zhang, H.; Gao, J.; Hopke, P.K. Chemical Characteristics of PM2.5 during a 2016 Winter Haze Episode in Shijiazhuang, China. *Aerosol Air Qual. Res.* **2017**, *17*, 368–380. [CrossRef]

114. Stein, A.F.; Draxler, R.R.; Rolph, G.D.; Stunder, B.J.B.; Cohen, M.D.; Ngan, F. Noaa's Hysplit Atmospheric Transport and Dispersion Modeling System. *Bull. Am. Meteorol. Soc.* **2015**, *96*, 2059–2077. [CrossRef]

115. United States Environmental Protection Agency. Risk Assessment Guidance for Superfund. Human Health Evaluation Manual Part A. 1989. Available online: https://www.epa.gov/risk/risk-assessment-guidance-superfund-rags-part (accessed on 2 April 2023).

116. US EPA. Risk Assessment Guidance for Superfund. In: Part A: Human Health Evaluation Manual; Part E, Supplemental Guidance for Dermal Risk Assessment; Part F, Supplemental Guidance for Inhalation Risk Assessment, vol. I. 2011. Available online: https://www.epa.gov/risk/risk-assessment-guidance-superfund-rags-part-f (accessed on 2 April 2023).

117. Khanna, I.; Khare, M.; Gargava, P. Health Risks Associated with Heavy Metals in Fine Particulate Matter: A Case Study in Delhi City, India. *J. Geosci. Environ. Prot.* **2015**, *3*, 72–77. [CrossRef]

118. Liu, X.; Zhai, Y.; Zhu, Y.; Liu, Y.; Chen, H.; Li, P.; Peng, C.; Xu, B.; Li, C.; Zeng, G. Mass Concentration and Health Risk Assessment of Heavy Metals in Size-Segregated Airborne Particulate Matter in Changsha. *Sci. Total Environ.* **2015**, *517*, 215–221. [CrossRef] [PubMed]

119. Chen, J.; Tan, M.; Li, Y.; Zheng, J.; Zhang, Y.; Shan, Z.; Zhang, G.; Li, Y. Characteristics of Trace Elements and Lead Isotope Ratios in PM2.5 from Four Sites in Shanghai. *J. Hazard. Mater.* **2008**, *156*, 36–43. [CrossRef] [PubMed]